The Ulm Fracture Healing Model

Supplementary Material to
Simulating Metaphyseal Fracture Healing in the Distal Radius

Lucas Engelhardt et al.

The *Ulm Fracture Healing Model*, was originally developed by Simon et al. [8]. Further improvements of the model can be attributed to Niemeyer et al. [5]. Inspired by the work of Pauwels, Claes and Heigele [3] depicted the hypothesis of mechano-regulated fracture healing by local hydrostatic and distorsional strain states. Later on, Ament and Hofer [1] gained the idea to implement a fuzzy logic to the differentiation process and applied a feedback control system to the healing process. Simon et al.[8] combined the idea of Claes and Heigele with the approach of Ament and Hofer to develop a more advanced, dynamic model of secondary fracture healing. Over time, further knowledge gained by various Ulm researchers was added. Special improvements were implemented by Niemeyer[4] focusing on the distraction osteogenesis process in the diaphysis.

Figure 1 shows the schematic procedure of the bone healing simulation. In the following, a short summary of every step is described.

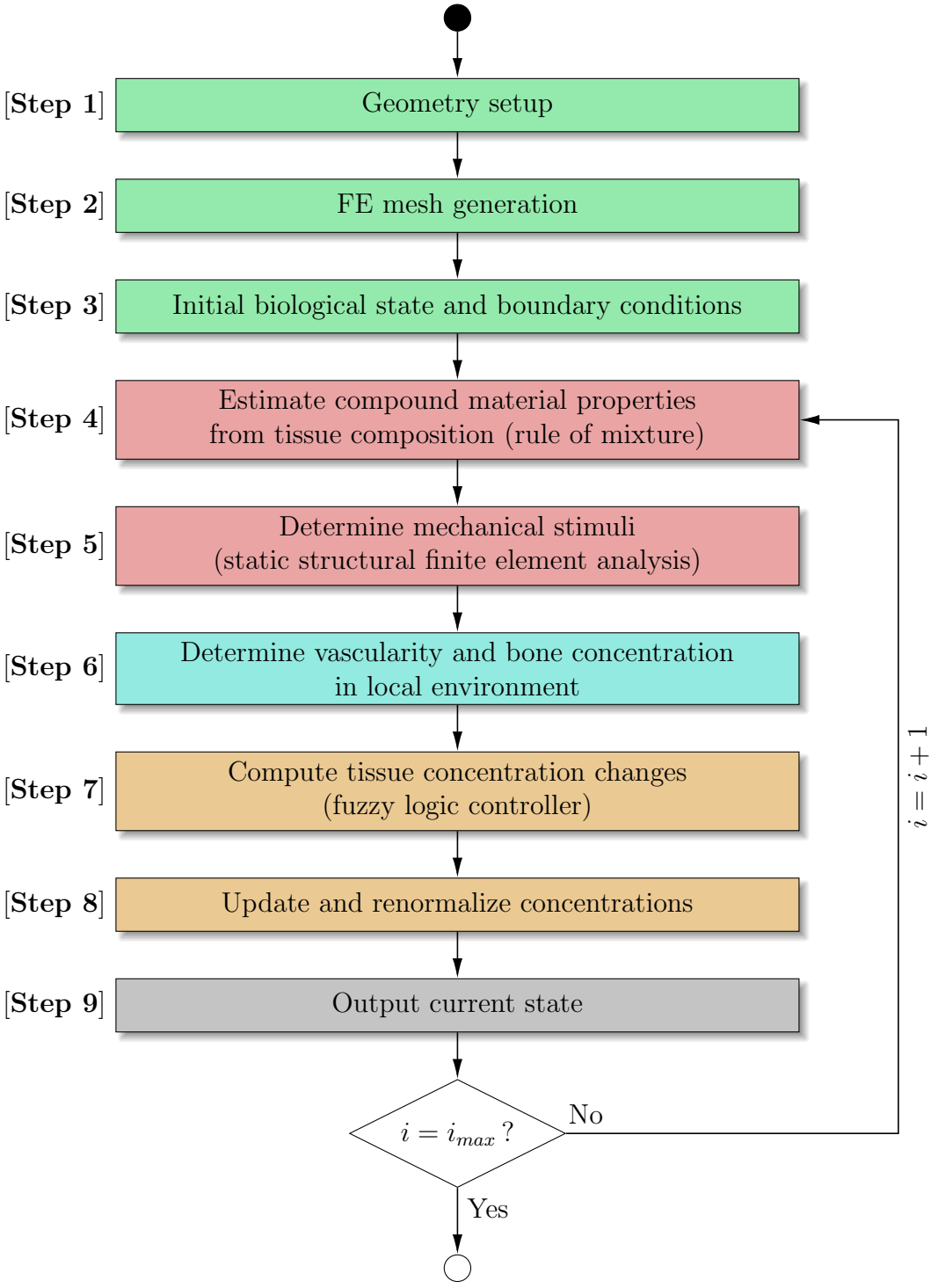

Figure 1: Schematic illustration of the bone healing simulation procedure; Figure is based on [4, Figure 1.28 on p. 47]

Step 1: The healing region $\Omega \subset \mathbb{R}^3$ is defined as a subset of the three-dimensional space.

Step 2: In order to perform a Finite Element Analysis (FEA), the healing area Ω is dicretized in *Finite Elements* (FE) $T_i \subset \mathbb{R}^3$.

Step 3: The healing domain Ω consists of a variety of different biological tissues, such as lamellar and woven bone, cartilage and soft tissue. Moreover, the vascularity is taken into account. Thus, five state variables are introduced, which represent the relative concentration of woven bone and lamellar bone, fibrocartilage, soft tissue and the degree of vascularity respectively. The concentration distributions are modeled in the form of five scalar fields

$$c_\tau : \Omega \times [0, \infty) \to [0, 1], \quad (r, t) \mapsto c_\tau(r, t)\,, \tag{1}$$

where $\tau \in \{lb, wb, c, s, v\} := \bigcup \tau$ (lb for lamellar bone, wb for woven bone, c for fibrocartilage, s for soft tissue and v for vascularity). Since the scalar fields c_{lb}, c_{wb}, c_c and c_s represent relative tissue concentrations, they have to sum up to one, i.e. $c_{lb}(r,t)+c_{wb}(r,t)+c_c(r,t)+c_s(r,t) \stackrel{!}{=} 1\ \forall r \in \Omega,\ \forall t \in [0,\infty)$ or, in other words, one of these variables is redundant and can be neglected - Simon et al. chose c_s. So, the biological state of the system is entirely expressed by the four *main* state variables c_{lb}, c_{wb}, c_c and c_v.

Considering the biological state at a fixed time point t the scalar field c_τ is assumed to be constant within an arbitrary FE T_i. Since c_τ is a piecewise constant function (step function), the biological state of element T_i is determined by four numbers $c_{lb,i}$, $c_{wb,i}$, $c_{c,i}$ and $c_{v,i}$ (compare Figure 2).

So, the biological state of the whole healing domain at a certain point in time can be represented by four vectors

$$\mathbf{c}_\tau \in [0,1]^n \subset \mathbb{R}^n, \quad \mathbf{c}_\tau \coloneqq \begin{pmatrix} c_{\tau,1} \\ c_{\tau,2} \\ \vdots \\ c_{\tau,n} \end{pmatrix} \tag{2}$$

for $\tau \in \{lb, wb, c, v\}$.

In order to describe the initial biological state of the entire healing domain, every element T_i needs to be assigned a mixture of the relative tissue concentrations and a relative vascularity at the beginning of the healing simulation. Furthermore, boundary conditions and other constraints are applied to the FE-model [8, p. 81].

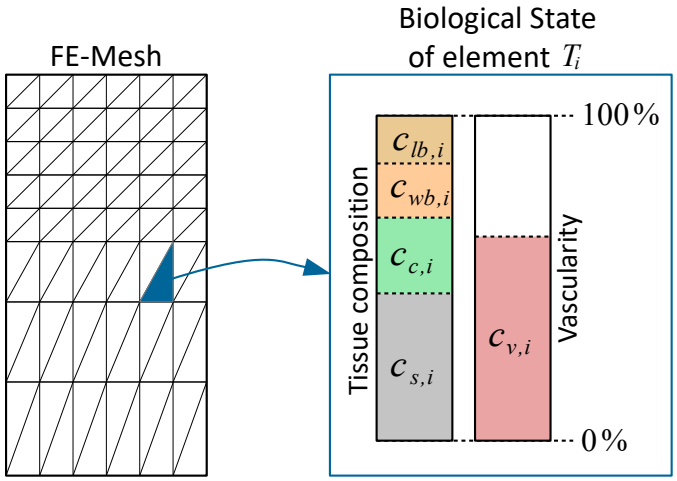

Figure 2: Left: Finite Element Mesh consisting of triangles (in 2D); Right: Biological state of element T_i determined by $c_{lb,i}$, $c_{wb,i}$, $c_{c,i}$, $c_{s,i} = 1 - c_{lb,i} - c_{wb,i} - c_{c,i}$ and $c_{v,i}$

Step 4: For the computation of the relevant strains, the mechanical properties of each element have to defined for the FEA. Hereby a linear isotropic material is described by the Young's modulus E_i and the Poisson's ratio ν_i. Since the elements in the healing simulation consist of an individual mixture of different materials, the mechanical properties for each element T_i is estimated individually. The approach used by Simon et al., the rule of mixture, determines those properties by weighting the corresponding pure tissues Young's modulus E_τ and the Poisson's ratio ν_τ with the relative tissue concentrations by

$$E_i = \sum_{\tau \in \bigcup \tau} E_\tau \cdot c_{\tau,i}^3 \qquad \text{and} \qquad \nu_i = \sum_{\tau \in \bigcup \tau} \nu_\tau \cdot c_{\tau,i}, \tag{3}$$

where E_τ and c_τ are the material parameters corresponding to the distinct tissue types. The expression originates from experimental data of Carter and Hayes [2], where the apparent compressive modulus of trabecular bone was analyzed and stated that the elastic modulus scales with the cube of the mineral density. We showed that this rule of mixture had problems [7], when mixing soft tissue with little hard tissue. Therefore, the tissues are ascendingly sorted ($E_{\tau_1} < E_{\tau_2} < ... < E_{\tau_N}$) and the resulting Young's modulus is calculated with:

$$E_i = E_{\tau_1} \cdot c_{\tau_1,i} + \sum_{j=2}^{N} \left(E_{\tau_j} - E_{\tau_{j-1}}\right) \cdot \left(\sum_{k=j}^{N} c_{\tau_k,i}\right)^3, \tag{4}$$

for N the number of tissue types.

Step 5: Through the FEAs resulting displacements, the mechanical stimuli acting on each element are deduced based on the tissue differentiation hypothesis of Pauwels [6] and Claes and Heigele [3]. Simon et al. distinguished between two invariants: A pure volumetric change (dilatational strain) and a pure shape distortion (distortional strain) as illustrated in Figure 3.

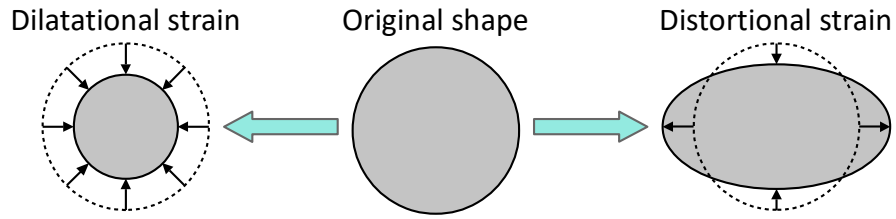

Figure 3: Left: Dilatational strain (pure volumetric change); Right: Distortional strain (pure shape distortion); Figure is based on [4].

Step 6: The tissue differentiation does not only depend on the biological state of the element itself and the mechanical stimuli acting on it, but also on the bone tissue concentration and relative vascularity within the local environment. For instance, bone formation can only take place on the surface of already existing bone tissue (appositional growth) and through angiogenesis new blood vessels form from pre-existing vessels. So, in order to predict the changes of tissue composition and perfusion, the bone tissue concentration and vascularity in the local environment of the considered element have to be taken into account.

Step 7: In this step, the current biological state serves as an input to a Fuzzy Logic Controller (see Figure 4). Herein the tissue differentiation processes are implemented and control the changes in vascularity, bone tissue concentration and cartilage concentration (see [4, p. 53-56, 326–333]).

In its current state, the model is able to capture the following biological processes:

- Intramembranous ossification: Fibrous connective tissue evolves into woven bone
- Chondrogenesis: Formation of cartilage out of connective tissue
- Endochondral ossification: Fibrocartilage transforms to bone tissue
- Bone maturation: Woven bone is slowly replaced by lamellar bone
- Tissue destruction: Too high mechanical loads may cause the destruction of existing cartilage or bone tissue

- Bone resorption: Existing bone tissue is replaced by soft tissue if the mechanical stimulation falls below a certain threshold.
- (Re-)Vascularization: Initially avascular tissue is revascularized over time.

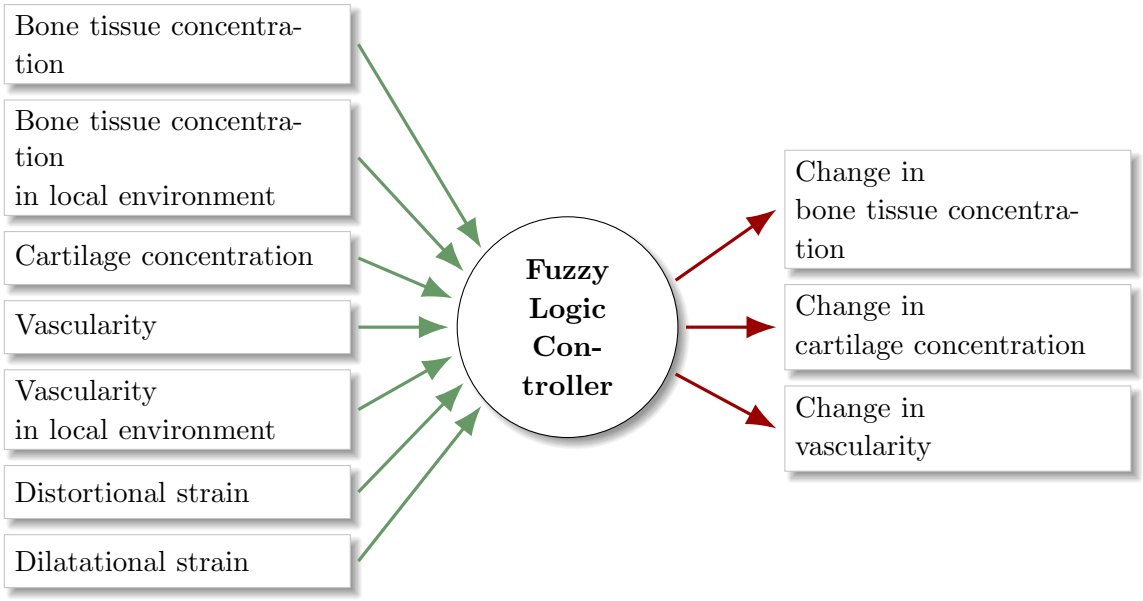

Figure 4: Tissue differentiation process modeled by Fuzzy Logic Controller; Left: Input; Right: Output; Figure is based on [4, Figure 1.32 on p. 54]

Step 8: To guarantee that the tissue concentrations sum up to 1 for each element i.e. $c_{b,i} + c_{c,i} + c_{s,i} \stackrel{!}{=} 1 \ \forall i \in \{1, ..., n\}$ (compare Figure 2), the concentration compositions are normalized For further information the reader is referred to [8, p. 82-85] and [4, p. 53-56, 90–94, 315–333].

Step 9: Finally, the simulation results, e.g. the current biological state of all FEs, is stored.

The Ulm Healing Model is a dynamic model. So, the procedure from step 4 to 9 is repeated several times, where each iteration represents a certain period of time, for instance one day. This is done by an explicit Euler scheme. When the iteration counter i reaches i_{max}, the simulation terminates.

Bibliography

[1] Ch Ament and E.P Hofer. "A fuzzy logic model of fracture healing". In: *Journal of biomechanics* 33.8 (2000), pp. 961–968. ISSN: 0021-9290. DOI: 10.1016/S0021-9290(00)00049-X.

[2] D. R. Carter and W. C. Hayes. "The compressive behavior of bone as a two-phase porous structure". In: *The Journal of bone and joint surgery. American volume* 59.7 (1977), pp. 954–962. ISSN: 0021-9355.

[3] L.E Claes and C.A Heigele. "Magnitudes of Local Stress and Strain along Bony Surfaces Predict the Course and Type of Fracture Healing". In: *Journal of Biomechanics* 32.3 (1999), pp. 255–266. DOI: 10.1016/s0021-9290(98)00153-5.

[4] Frank Niemeyer. "Simulation of Fracture Healing". [dissertation]. Ulm: Ulm University, 2013.

[5] Frank Niemeyer et al. "Simulating lateral distraction osteogenesis". In: *PloS one* 13.3 (2018), e0194500. DOI: 10.1371/journal.pone.0194500.

[6] Friedrich Pauwels. "Grundriß einer Biomechanik der Frakturheilung [in german]". In: *Gesammelte Abhandlungen zur funktionellen Anatomie des Bewegungsapparates*. Springer Berlin Heidelberg, 1965, pp. 139–182. DOI: 10.1007/978-3-642-86841-2_2.

[7] M. Pietsch et al. "Modelling the Fracture-healing Process as a Moving-interface Problem using an Interface-capturing Approach". In: *Computer Methods in Biomechanics and Biomedical Engineering* (2018), accepted. DOI: 10.1080/10255842.2018.1487554.

[8] U. Simon et al. "A Numerical Model of the Fracture Healing Process that Describes Tissue Development and Revascularisation". In: *Computer Methods in Biomechanics and Biomedical Engineering* 14.1 (2011), pp. 79–93. DOI: 10.1080/10255842.2010.499865.